



Stability of cytochromes *c'* from psychrophilic and piezophilic *Shewanella* species: implications for complex multiple adaptation to low temperature and high hydrostatic pressure

Asako Suka¹ · Hiroya Oki² · Yuki Kato¹ · Kazuki Kawahara² · Tadayasu Ohkubo² · Takahiro Maruno³ · Yuji Kobayashi³ · Sotaro Fujii¹ · Satoshi Wakai⁴ · Lisa Lisdiana^{1,5} · Yoshihiro Sambongi¹

Received: 19 November 2018 / Accepted: 13 January 2019 / Published online: 28 January 2019
© Springer Japan KK, part of Springer Nature 2019

Abstract

The stability of dimeric cytochrome *c'* from a thermophile, as compared with that of a homologous mesophilic counterpart, is attributed to strengthened interactions around the heme and at the subunit–subunit interface, both of which are molecular interior regions. Here, we showed that interactions in the equivalent interior regions of homologous cytochromes *c'* from two psychrophiles, *Shewanella benthica* and *Shewanella violacea* (SBCP and SVCP, respectively) were similarly weakened as compared with those of the counterparts of psychrophilic *Shewanella livingstonensis* and mesophilic *Shewanella amazonensis* (SLCP and SACP, respectively), and consistently the stability of SVCP, SLCP, and SACP increased in that order. Therefore, the stability of cytochromes *c'* from the psychrophile, mesophile, and thermophile is systematically regulated in their molecular interior regions. Unexpectedly, however, the stability of SBCP was significantly higher than that of SVCP, and the former had additional molecular surface interactions. Collectively, SBCP had weakened interior interactions like SVCP did, but the former was stabilized at the molecular surface as compared with the latter, implying complex multiple adaptation of the proteins because the psychrophilic sources of SBCP and SVCP are also piezophilic, thriving in deep-sea extreme environments of low temperature and high hydrostatic pressure.

Keywords Cytochrome *c'* · Protein stability · Piezophile · Psychrophile · *Shewanella*

Abbreviations

CD Circular dichroism

SACP *Shewanella amazonensis* cytochrome *c'*

SBCP *Shewanella benthica* cytochrome *c'*

SLCP *Shewanella livingstonensis* cytochrome *c'*

SVCP *Shewanella violacea* cytochrome *c'*

Introduction

The thermal stability of a series of homologous proteins correlates with the optimal growth temperatures of the source organisms from mesophiles growing at more than 20 °C to thermophiles growing at more than 45 °C (Gromiha et al. 1999; Akanuma et al. 2013; Sambongi et al. 2002). Therefore, the stability of the proteins appears to be related directly to the source's natural temperature environment at more than 20 °C.

Cytochrome *c'*, the target protein in this study, is a heme protein found in a variety of Gram-negative bacteria (Ambler et al. 1991). It forms homo dimer, where each monomer has a four α -helix bundle structure containing a covalently bound penta-coordinate heme (Moore 1991). We have so far investigated the thermal stability of three cytochromes *c'* from one thermophile, *Hydrogenophilus thermoluteolus*,

Communicated by A. Oren.

✉ Yoshihiro Sambongi
sambongi@hiroshima-u.ac.jp

- ¹ Graduate School of Biosphere Science, Hiroshima University, Higashi-Hiroshima, 1-4-4 Kagamiyama, Hiroshima 739-8528, Japan
- ² Graduate School of Pharmaceutical Sciences, Osaka University, 1-6 Yamadaoka, Suita, Osaka 565-0871, Japan
- ³ Graduate School of Engineering, Osaka University, 2-1 Yamadaoka, Suita, Osaka 565-0871, Japan
- ⁴ Graduate School of Science, Technology, and Innovation, Kobe University, 1-1 Rokkodai-cho, Nada-ku, Kobe 657-8501, Japan
- ⁵ Department of Biology, Universitas Negeri Surabaya, Kampus Unesa Ketintang, Surabaya 60231, Indonesia

which optimally grows at 52 °C (Goto et al. 1977) and two mesophiles, *Shewanella amazonensis* and *Allochrodatum vinosum*, which optimally grow at 37 and 25 °C, respectively (Venkateswaran et al. 1998; Holm and Vennes 1970). These three cytochromes *c'* exhibited different thermal stability, which was in accordance with the optimal growth temperatures of the source bacteria (Inoue et al. 2011; Fujii et al. 2013; Kato et al. 2015). Therefore, cytochromes *c'* show a relationship between protein stability and bacterial growth temperature when they originate from mesophiles and thermophiles, as observed in the other proteins (Gromiha et al. 1999; Akanuma et al. 2013; Sambongi et al. 2002), but it remains unknown whether this relationship applies to cytochromes *c'* from psychrophiles.

Fortunately, a highly homologous series of cytochromes *c'* is found in *Shewanella* species, which include both psychrophiles and mesophiles. In this study, the stability and structure of four homologous cytochromes *c'* from three psychrophilic and one mesophilic *Shewanella* species were compared. The cytochromes *c'* used in this study were SBCP, SVCP, SLCP, and SACP, isolated from *Shewanella benthica*, *Shewanella violacea*, *Shewanella livingstonensis*, and *Shewanella amazonensis*, which optimally grow at 4, 8, 20, and 37 °C, respectively, under 0.1 MPa conditions (Kato et al. 1995; Kulakova et al. 1999; Venkateswaran et al. 1998). In particular, the amino acid sequence identity between SBCP and SVCP is strikingly high, 92%, and their psychrophilic source bacteria, *S. benthica* and *S. violacea*, are also both piezophiles, being isolated from extremely deep-sea environments, i.e., at more than 5000 m depth. In spite of the environmental similarity between *S. benthica* and *S. violacea*, SBCP was unexpectedly more stable than SVCP, and thus the both are examples regarding complex multiple adaptation of proteins to low temperature and high hydrostatic pressure.

Materials and methods

Gene sequencing and cloning

Chromosomal DNA of *S. benthica* DB6705, *S. violacea* DSS12, and *S. amazonensis* SB2B was prepared as described previously (Takenaka et al. 2010; Masanari et al. 2014), which were then used to amplify the SBCP, SVCP, and SACP genes to confirm their sequences. The PCR primers used for the gene amplification are listed in Table 1. The SLCP gene sequence was kindly provided by Dr. Kurihara of Kyoto University, Japan.

The genes encoding for the mature SBCP, SVCP, SLCP, and SACP proteins fused with the *Pseudomonas aeruginosa* cytochrome *c*₅₅₁ signal gene sequence at the N-terminal region were synthesized using optimized codons for

Table 1 Primers used in this study for gene sequencing and mutagenesis experiments

Primer		5' to 3'
For sequencing		
SBCP	Fw	tagaatacaataccgagtggaacatcac
	Rv	ggagttcatcaggctctagccttttta
SVCP	Fw	gcgaattcataattcgtgagagcaatgca
	Rv	cgctcgacttaactcttctgtagacgtc
SACP	Fw	cttcggttacaatgactgtctttgcgtct
	Rv	tcaggcactgtaacgggtgatactgaaata
For mutation		
SBCP A43T	Fw	atthttACCatgcgtgcacagaatgtt
	Rv	acgcatGGTaaaaattcgtatcaaa
SBCP P62Q	Fw	tttattCAGggtagcagcagggtgaa
	Rv	gctaccCTGaataaaacctccagcgg
SBCP K87V	Fw	aaaatgGTGaccctcaggataatgca
	Rv	cagggtCACatttggcatcaaaatc

The nucleic acid residues in upper case are those that were mutated

Escherichia coli by a manufacturer (Thermo Fisher Scientific). The fused genes were inserted into the pKK223-3 vector at the *EcoRI* and *SalI* restriction sites under the control of a *tac* promoter.

Protein expression and purification

The plasmids carrying the genes for SBCP, SVCP, SLCP, and SACP were transformed into *E. coli* JCB387 containing the pEC86 plasmid carrying the genes for cytochrome *c* maturation (*ccmABCDEFGH*). *E. coli* JCB387 cells expressing cytochromes *c'* were initially pre-cultured in liquid LB medium containing 100 µg/mL ampicillin and 30 µg/mL chloramphenicol. These LB pre-cultures (2 mL) were inoculated into 20 mL LB medium containing the same antibiotics, followed by shaking at 37 °C for 3 h. After this pre-cultivation, 20 mL LB medium was inoculated into 2 L minimal medium (Sambongi and Ferguson 1994) containing the same antibiotic, 0.8% (v/v) glycerol, and 50 µg/mL 5'-aminolevulinic acid in a 5 L Sakaguchi flask, and then the cells were grown at 37 °C with shaking for 21 h. The periplasmic protein fractions of the resulting cells were obtained by the cold osmotic shock method as described previously (Sambongi et al. 1996).

The periplasmic protein fractions containing the SBCP and SVCP proteins were dialyzed against 10 mM Tris-HCl buffer (pH 8.0) at 4 °C containing 100 mM NaCl to prevent protein aggregation. These fractions were then loaded onto a DEAE column (GE Healthcare, Tokyo) that had been equilibrated with the same buffer. The fractions containing cytochrome *c'* proteins were eluted with the same buffer containing 300 mM NaCl. The cytochrome *c'* fractions were dialyzed against the same buffer containing

100 mM NaCl, and then loaded onto a HiTrap Q column (GE Healthcare, Tokyo) that had been equilibrated with the same buffer. The cytochrome *c'* fractions were eluted with the same buffer using the NaCl concentration gradient method (100–500 mM), and then dialyzed against 25 mM sodium acetate buffer (pH 5.0) at 4 °C containing 100 mM NaCl. The fractions were further loaded onto a HiTrap SP column (GE Healthcare, Tokyo) that had been equilibrated with the same buffer. The cytochrome *c'* fractions were eluted with the same buffer using the NaCl concentration gradient method (100–300 mM), followed by loading onto a Superdex™ 75 column (GE Healthcare, Tokyo) equilibrated and eluted with 10 mM Tris-HCl buffer (pH 7.0) containing 150 mM NaCl at 4 °C.

The SLCP and SACP proteins were purified by the similar method as for SBCP and SVCP without the addition of 100 mM NaCl to the dialyzing buffer before the column chromatography procedure. The protein concentrations were determined spectrophotometrically using an extinction coefficient of 205 nm due to the peptide bond (Scopes 1974). The purity of the cytochrome *c'* proteins was checked by sodium dodecyl sulfate polyacrylamide gel electrophoresis.

Spectral analysis of the recombinant proteins

The recombinant SBCP, SVCP, SLCP, and SACP proteins were air-oxidized or reduced with a grain of sodium dithionite. Visible absorption spectra (350–700 nm) of the oxidized and reduced SBVP, SVCP, SLCP, and SACP protein solutions (6 μM) in 100 mM potassium phosphate buffer (pH 7.0) at 25 °C were obtained with a JASCO V-730-Bio spectrometer at 25 °C (Jasco, Tokyo).

Sedimentation velocity analysis of the SBCP, SVCP, SLCP, and SACP protein solutions was performed with a Beckman Optima XL-I analytical ultracentrifuge (Beckman Coulter, California) equipped with a 4-hole An60 Ti rotor at 20 °C using 12-mm double-sector charcoal-filled Epon centerpieces with quartz windows to determine their subunit compositions. Each protein solution (5 μM) was dissolved in 10 mM Tris-HCl buffer (pH 7.5) containing 100 mM NaCl. Data were collected using absorbance optics at 390–400 nm with a radial increment of 0.003 cm and at a rotor speed of 42,000 rpm. The distribution of sedimentation coefficients (*S*) was analyzed using the continuous *c(s)* distribution model in the SEDFIT version 14.1 program (Schuck 2000), as previously reported (Fujii et al. 2017). The positions of the meniscus and cell bottom were floated during the fitting. The range of sedimentation coefficients for fitting was 0–15*S* with a resolution of 300.

Circular dichroism (CD) spectra (190–260 nm) of the oxidized SBCP, SVCP, SLCP, and SACP protein solutions (20 μM) in 100 mM potassium phosphate buffer (pH 7.0)

were obtained with a JASCO J-820 CD spectrometer at 25 °C (Jasco, Tokyo).

Crystallization

The purified SBCP and SVCP protein solutions were dialyzed against milliQ water containing 100 mM NaCl, and then concentrated to ~15 mg/mL. The initial crystallized conditions were screened by the hanging-drop vapor diffusion method at 4 °C using Crystal Screens I and II (Hampton Research, California). The solution drops for crystallization were prepared by mixing 2 μL of protein solution and 1 μL of reservoir solution, followed by equilibration against 400 μL of a reservoir solution. The SBCP protein was crystallized using a reservoir solution consisting of 100 mM *N*-cyclohexyl-3-aminopropanesulfonic acid/sodium hydroxide buffer (pH 10.5) and 30% (v/v) polyethylene glycol 400 within 5 days, and the SVCP protein was also crystallized using a reservoir solution consisting of 100 mM *N*-cyclohexyl-3-aminopropanesulfonic acid/sodium hydroxide buffer (pH 9.4) and 26% (v/v) polyethylene glycol 400 within 7 days.

X-ray diffraction

The X-ray diffraction experiments on the SBCP and SVCP crystals were carried out on a Rigaku Micromax-007 rotating anode X-ray generator with a Cu target and an R-AXIS IV⁺⁺ imaging plate detector (Rigaku, Tokyo). The SBCP and SVCP crystals were flash-cooled at –173 °C in a stream of cold nitrogen, using the following cryoprotectant solution: 100 mM *N*-cyclohexyl-3-aminopropanesulfonic acid/sodium hydroxide buffer (pH 10.5) and 30% (v/v) polyethylene glycol 400. A total of 210 images was collected for each of the SBCP and SVCP crystals, respectively, at camera lengths of 120 mm for SBCP and 150 mm for SVCP and an oscillation angle of 1.0°. The SBCP and SVCP crystals diffracted to maximal resolutions of 1.71 and 2.14 Å, respectively (Table 2). The diffraction data sets were processed using the CrystalClear program (Rigaku, Japan). The SBCP and SVCP crystals belonged to space groups $C2_1$ ($a = 72.67$ Å, $b = 52.47$ Å, $c = 50.93$ Å) and $P2_1$ ($a = 44.75$ Å, $b = 69.71$ Å, $c = 45.60$ Å), respectively. The Matthews coefficient values were 2.45 Å³/Da and 2.27 Å³/Da, respectively, which correspond to solvent contents of 49.9 and 42.7%, respectively (Matthews 1968).

Molecular replacement and structure refinement

The structures of SBCP and SVCP were determined by the molecular replacement method using the Phaser program included in the PHENIX software suite (McCoy et al. 2007), and the crystal structure of *Shewanella*

Table 2 Data collection, phasing and refinement statistics for the SBCP and SVCP crystals

Data collection	SBCP	SVCP
Detector	R-AXIS IV ⁺⁺	R-AXIS IV ⁺⁺
Wavelength (Å)	1.540	1.540
Exposure time (min)	5.0	12.0
Oscillation width (°)	1.0	1.0
Resolution range (Å) ^a	37.34–1.71 (1.77–1.71)	37.49–2.14 (2.22–2.14)
Space group	C2 ₁	P2 ₁
Unit-cell parameters(Å, °)		
<i>a</i> , <i>b</i> , <i>c</i> (Å)	72.67, 52.47, 50.93	44.75, 69.71, 45.60
α , β , γ (°)	90.0, 132.85, 90.0	90.0, 112.19, 90.0
Total measured reflections	61,669	61,138
Unique reflections	15,047	14,639
R_{merge}^b	0.061 (0.214)	0.096 (0.451)
Average $I/\sigma(I)$	16.9 (3.8)	7.8 (2.7)
Completeness (%)	98.5 (85.6)	99.9 (10.0)
Refinement		
Resolution range (Å)	21.26–1.71 (1.77–1.71)	25.20–2.14 (2.22–2.14)
R_{work}^c	0.166	0.215
R_{free}^d	0.198	0.272
Overall B-factors	21.0	48.0
R. m. s. deviations		
Bond length (Å)	0.006	0.009
Bond angle (°)	0.884	1.078
Ramachandran plot statistics		
Most favoured (%)	99.2	99.2
Disallowed (%)	0.00	0.00

^aValues in parentheses were for the highest resolution shell

^b $R_{\text{merge}} = \sum |I_h - \langle I_h \rangle| / \sum I_h$, where $\langle I_h \rangle$ is the average intensity of reflection *h* and symmetry-related reflections

^c $R_{\text{work}} = \sum ||F_o| - |F_c|| / \sum |F_o|$, where F_o and F_c are the observed and calculated structure factor amplitudes, respectively

^d $R_{\text{free}} = R_{\text{work}}$ is calculated using 10% of the reflection data chosen randomly and set aside at the start of refinement

frigidimarina cytochrome *c'* (PDB ID: 4ULV, Manole et al. 2015) was applied as a search model, which showed 68 and 70% amino acid sequence identity with SBCP and SVCP, respectively. The structural refinement, manual model building, and addition of water molecules were carried out using the phenix.refine and Coot programs (Adams et al. 2010; Emsley and Cowtan 2004). Finally, the refinement converged to an R_{work} of 0.166 and an R_{free} of 0.198 for SBCP, and an R_{work} of 0.215 and an R_{free} of 0.272 for SVCP. The geometry of the final SBCP and SVCP structure models was checked using the MolProbity program based on Ramachandran plot statistics (Table 2) (Chen et al. 2010). The final coordinates of SBCP and SVCP have been deposited in the Protein Data Bank (PDB ID: 6A3K and 6A3L).

Three-dimensional model structures of SLCP and SACP

As the amino acid sequence of SLCP from psychrophilic *S. livingstonensis* was 100% identical to that of similarly psychrophilic *S. frigidimarina* cytochrome *c'* that had been determined through X-ray analysis (PDB ID: 4ULV, Manole et al. 2015), the three-dimensional structure of *S. frigidimarina* cytochrome *c'* was adopted as a model structure of SLCP in this study. The three-dimensional model structure of SACP could be successfully simulated using the crystal structure of *S. frigidimarina* cytochrome *c'* (PDB ID: 4ULV) as a template with the SWISS-MODEL workplace (Biasini et al. 2014). These SLCP and SACP three-dimensional model structures were used for comparison with

X-ray crystal structures of SBCP and SVCP experimentally obtained in this study.

Thermal denaturation experiment

Thermal denaturation of the SBCP, SVCP, SLCP, and SACP proteins was measured as circular dichroism (CD) spectra in a pressure-proof cell compartment (Jasco, Tokyo) attached to a CD spectrometer. The protein solutions (20 μ M) were dialyzed against 100 mM potassium phosphate buffer (pH 7.0) at 25 °C. The temperature-dependent CD ellipticity changes at 222 nm were monitored in a cuvette of 1-mm path length from 25 to 100 °C at intervals of 0.5 °C and a heating rate of 1.0 °C/min under 0.9 MPa pressure conditions.

The raw data were subjected to nonlinear least-squares fitting as described previously (Uchiyama et al. 2004). The data points were corrected for the slopes of the baselines for the native and denatured forms, and were normalized to calculate the fraction of protein denatured. The fraction denatured was plotted as a function of temperature, and the resulting thermal denaturation curves were used to determine the temperature at the midpoint of the transition (T_m).

Mutagenesis

Plasmids for expression of SBCP variants were prepared with a PrimeSTAR Mutagenesis Basal kit (TaKaRa Bio, Shiga), which had been applied to the wild-type gene inserted in the pKK223-3 vector. Ala-43, Pro-62, and Lys-87 in SBCP were separately substituted with Thr, Gln, and Val, respectively, which were the corresponding residues in SVCP. The primers used for the mutagenesis experiments are listed in Table 1. The correct introduction of mutations was confirmed by DNA sequencing. All the resulting plasmids were used for the expression of SBCP variants in *E. coli* JCB387 as described for the wild-type protein.

Results and discussion

Quality of the recombinant proteins

To confirm the quality of the recombinant proteins used in this study, the following analyses were performed. The sequence of SBCP gene from *S. benthica* DB6705 was determined using PCR primers constructed from the genome sequence of *S. benthica* KT99 that had been deposited in NCBI (Lauro et al. 2013). From the present sequencing results, we realized that three amino acid residues differed in the mature SBCP sequence from the two strains; the Glu-47, Ala-88, and Arg-105 residues of the KT99 strain were replaced with Gln, Thr, and Lys in the DB6705 strain, respectively. Here we adopted the strain DB6705 sequence

(Accession number: LC406697), and the experiments in this study were carried out using the SBCP protein from that strain. The SVCP and SACP gene sequences obtained in this study, respectively, were confirmed to be 100% identical to the genome sequences that had been deposited.

The N-terminal sequences of the recombinant SBCP, SVCP, SLCP, and SACP proteins were determined to be Ser-Asn-Phe-Lys-Glu-, Gly-Asn-Phe-Lys-Glu-, Asn-Asn-Phe-Glu-Glu-, and Asn-Asn-Phe-Glu-Ser-, respectively, which appeared to be authentic N-terminal sequences. Therefore, the signal peptide of the *P. aeruginosa* cytochrome c_{551} was successfully cleaved from these mature proteins in the *E. coli* cells.

Visible absorption spectra of the oxidized SBCP, SVCP, SLCP, and SACP proteins showed typical peaks at 339–400 and 635–637 nm, and those of the reduced forms showed peaks at 427 and 545–549 nm (Fig. 1a). These results indicated that these proteins have penta-coordinate heme, as reported for other authentic mesophilic and thermophilic cytochromes c' (Inoue et al. 2011; Kato et al. 2015).

The subunit compositions of the four cytochromes c' were determined through an analytical ultracentrifugation experiment. The S values of SBCP, SVCP, SLCP, and SACP were 2.7 S with a population of more than 91%, the calculated molecular mass values being 31.1, 31.3, 30.5, and 29.5 kDa, respectively (Fig. 1b). All theoretical molecular masses of these cytochromes c' were 14 kDa, calculated as a single subunit, indicating that these 2.7 S peaks indicated dimeric structures. However, parts of the populations showed monomeric structures reflected by smaller S values (~0.9–1.1) than those of the dimeric structures, indicating that these four proteins each existed predominantly as a dimer with a small quantity of monomer.

The CD spectra of the SBCP, SVCP, SLCP, and SACP proteins showed specific negative peaks at 208 and 222 nm (Fig. 1c), indicating that they contain an α -helical structure. The results obtained on the present spectral analyses indicated that the heme environment, subunit composition, and secondary structure were quite similar in these four recombinant proteins, which were used in the following experiments.

Overall structures of SBCP and SVCP

As to the crystal structures of cytochromes c' from psychrophilic *Shewanella* species, that of shallow-sea *S. frigidimarina* cytochrome c' (PDB ID: 4ULV, Manole et al. 2015) is only available, and those of deep-sea *Shewanella* species remain unknown. Here, the X-ray crystal structures of SBCP and SVCP from deep-sea *Shewanella* species were first determined at 1.71 and 2.14 Å resolutions, respectively (Fig. 2a), by the molecular replacement method (McCoy et al. 2007) using the crystal structure of *S. frigidimarina* cytochrome c' , which exhibited 68 and 70% amino acid

Fig. 1 Characteristics of SBCP, SVCP, SLCP, and SACP with spectral techniques. **a** Visible absorption spectra of the four proteins. Red and black solid lines represent the spectra of oxidized and reduced proteins, respectively. Relevant wavelengths are indicated by arrows. **b** Distribution of the sedimentation coefficients of the four proteins on analytical ultracentrifugation analysis. The data are fitted using continuous $c(s)$ distribution method with the SEDFIT program. **c** CD spectra of the four proteins. Relevant wavelengths are indicated by arrows

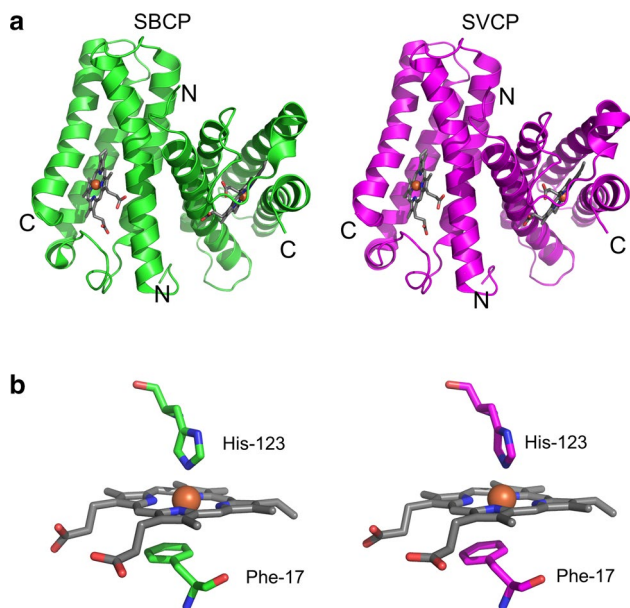
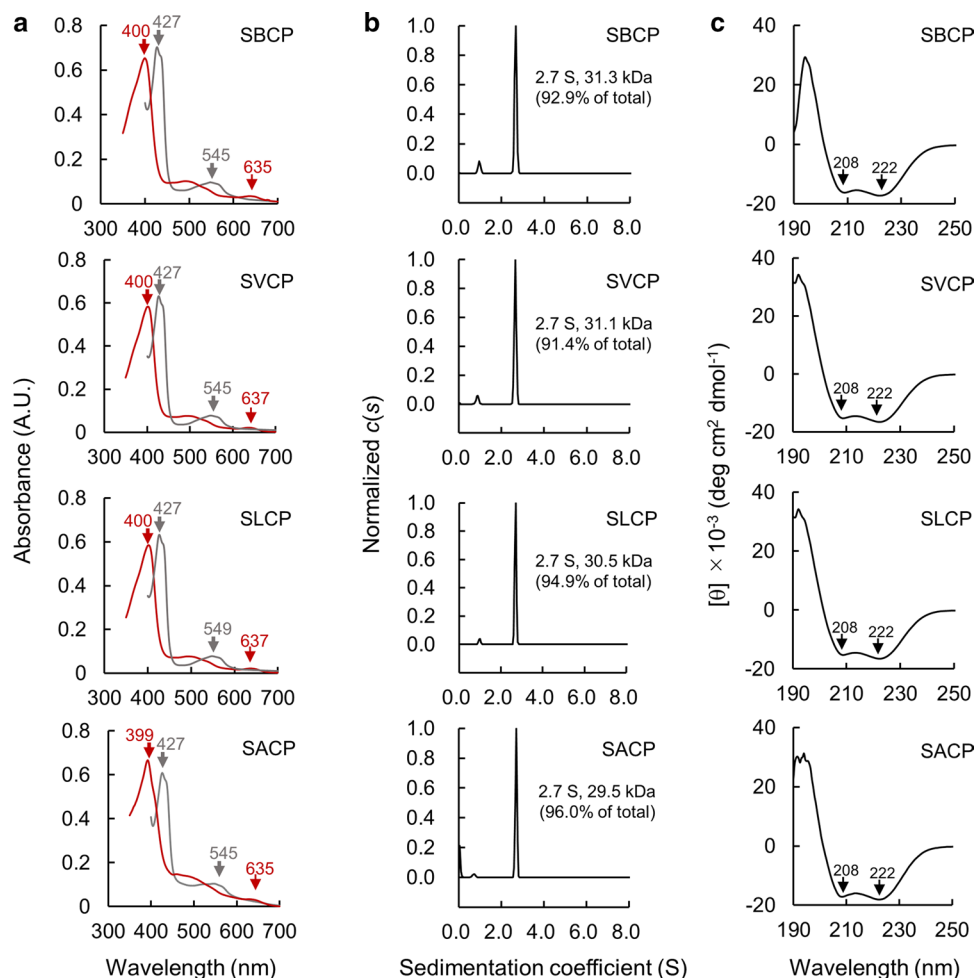


Fig. 2 Structure comparison between SBCP (green) and SVCP (violet). **a** Overall structures. The main chain and heme structures are shown as ribbon and stick models, respectively. The N- and C-termini of each subunit are also indicated. **b** Heme environment

sequence identity with SBCP and SVCP, respectively. The two main chain structures superimposed well, the root-mean-square-deviation value being 0.42 Å. They consisted of homo dimeric subunits where each monomer had a four α -helix bundle structure, as observed in the other cytochrome c' proteins. Around the heme in SBCP and SVCP, the side chains of His-123 residues were coordinated to the heme iron at the proximal site and those of Phe-17 were located at the vacant sixth distal site parallel with the heme (Fig. 2b). All these structural results for SBCP and SVCP are consistent with those of spectral analyses described above.

Stability prediction through the structure comparison

The X-ray crystal structures of SBCP and SVCP obtained in this study were compared with the three-dimensional model structures of SLCP and SACP (see “Materials and methods”) to predict their stability. Previously we found that the stability of a dimeric cytochrome c' from a thermophile, as compared with that of a homologous mesophilic counterpart, is due to strengthened interactions around the heme and at the

subunit–subunit interface, both of which are in molecular interior regions (Fujii et al. 2017; Yamane-Koshizawa et al. 2018). We here examined whether interactions in molecular interior regions differed in the SBCP, SVCP, SLCP, and SACP proteins from psychrophiles to a mesophile to predict their stability differences.

Around the heme, Asp-70 in SACP formed a hydrogen bond with the propionate group of the heme, whereas Glu-70 in SBCP, SVCP, and SLCP did not (Fig. 3a). The Leu-89 residues in SBCP and SVCP hydrophobically interacted with the heme, and the corresponding Phe-89 residues in SLCP and SACP also interacted hydrophobically with the heme (Fig. 3a). The Phe-89 residues in SLCP and SACP appeared to fill the space around the heme more favorably than those in SBCP and SVCP, which may strengthen the interaction in SLCP and SACP. Furthermore, at the subunit–subunit interface, only one hydrogen bond between the Ser-15 residues in the two subunits was formed in SBCP and SVCP, while two between the Tyr-22 and Glu-58 residues, and three between the Ser-15 residues and the Tyr-22 and Glu-58 residues were formed in SLCP and SACP, respectively (Fig. 3b). These results indicated that the interactions in the molecular interior regions of SBCP and SVCP were similarly weakened as compared with those of SLCP and SACP, consistent with our previous findings for the cytochrome *c'* proteins from

mesophiles and a thermophile where thermophilic one had strengthened molecular interior as compared with mesophilic ones (Fujii et al. 2017).

Validation of stability prediction through thermal stability analysis

To validate the stability prediction through structural comparison among SBCP, SVCP, SLCP, and SACP described above, thermal denaturation experiments were carried out by means of CD spectral measurement. The normalized data for CD spectral changes at 222 nm during the thermal denaturation were plotted as a function of temperature (Fig. 4a). The values for the transition temperatures (T_m) during thermal denaturation of the SBCP, SVCP, SLCP, and SACP proteins were 55.5 ± 0.0 , 48.3 ± 0.4 , 51.3 ± 0.7 , and 63.7 ± 0.0 °C, respectively, the mean and standard deviation values being obtained for three independent measurements. Among the four proteins, the T_m values of SVCP, SLCP, and SACP revealed a clear correlation with the optimal growth temperatures of the source bacteria (Fig. 4b), as predicted from their structures in the molecular interior regions (Fig. 3). Unexpectedly, however, the T_m value of SBCP was significantly higher than that of SVCP (Fig. 4b), although the interactions in the molecular interior regions of

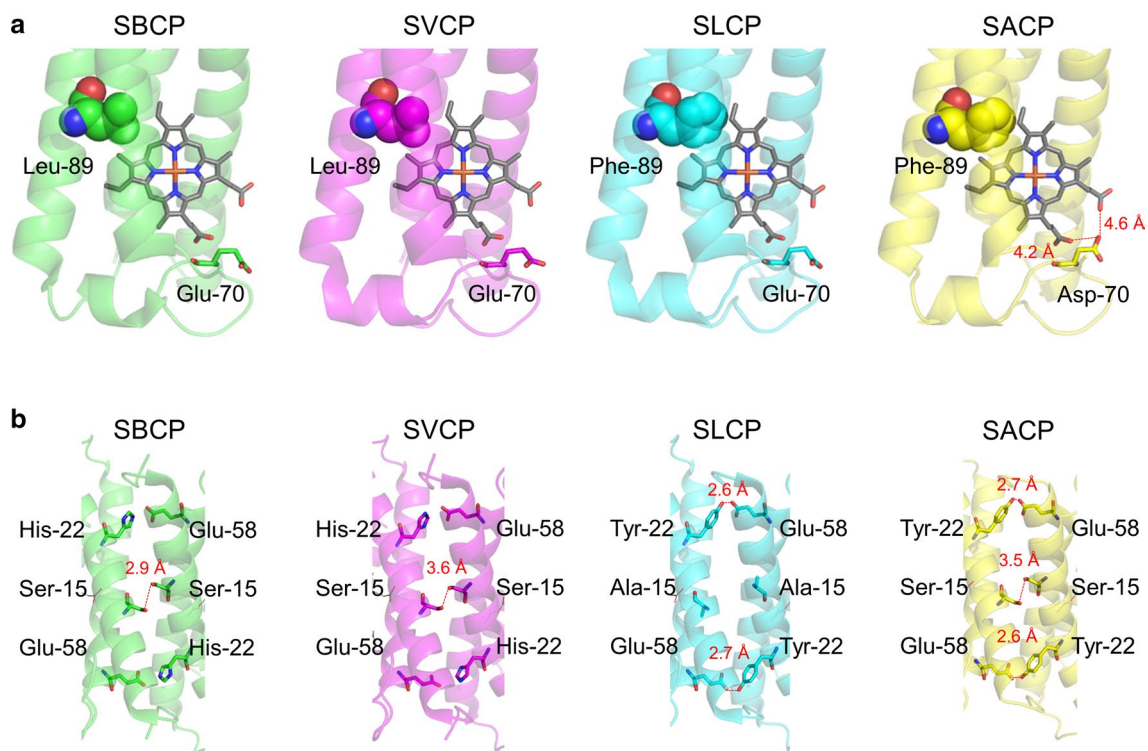


Fig. 3 Structural comparison among SBCP (green), SVCP (violet), SLCP (cyan), and SACP (yellow). **a** Interactions around the heme. Hydrophobic and other relevant residues are shown as sphere and

stick models, respectively. **b** Interactions at the subunit–subunit interface. In both panels, the hydrogen bonds formed are indicated by red dotted lines

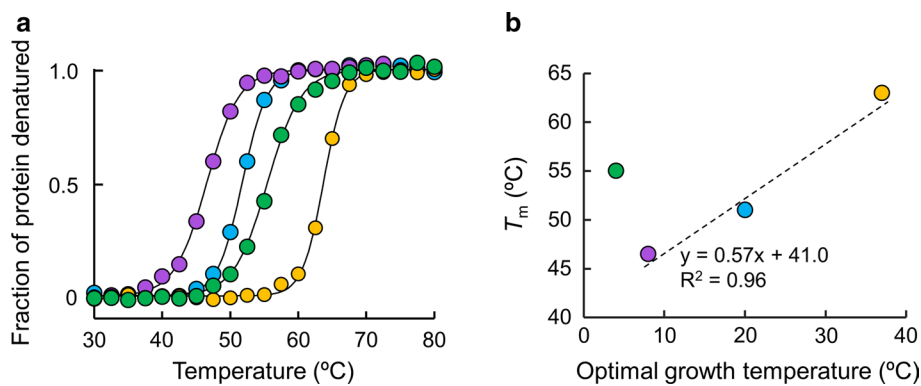


Fig. 4 Thermal stability of four *a* *Shewanella* cytochromes *c'*. Thermal denaturation, measured as CD spectra. The fractions of representative raw data are plotted at temperature interval of 2.5 °C for SVCP (violet circles), SLCP (cyan circles), SBCP (green circles), and SACP (yellow circles). The fitting curves are also shown. **b** Rela-

tionship between optimal growth temperatures of *Shewanella* species at 0.1 MPa and the T_m values of cytochromes *c'*. The symbol colors used are same as those in panel **a**. The dashed line shows the fitted linear line obtained using the data for SACP, SLCP, and SVCP

SBCP were similar to those in SVCP. There must be some other clues in their structures for this stability difference.

Structural insights into the stability difference between SBCP and SVCP

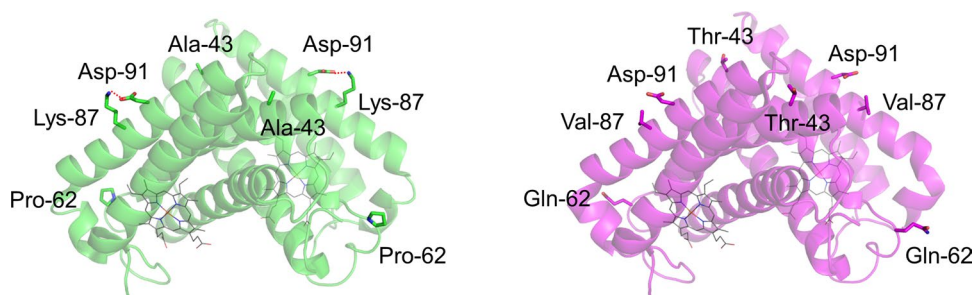
Although SBCP and SVCP significantly differed in the stability, the two proteins exhibited 92% sequence identity, only ten out of 129 residues differed. Ser-1, Ala-43, Gln-47, Pro-62, Gln-66, Glu-68, Glu-78, Lys-87, Thr-88, and Gln-114 in SBCP were substituted by Gly-1, Thr-43, Glu-47, Gln-62, Leu-66, Asp-68, Asp-78, Val-87, Ser-88, and Lys-114 in SVCP, respectively. Among these differences, the SBCP Ala-43 residue was located in an α -helix region, in the interior of molecule (Fig. 5), and its helix conformation tendency (Chou and Fasman 1978) is higher than that of the corresponding Thr-43 in SVCP. The Pro-62 residue of SBCP was located in a loop on the molecular surface, which may stabilize its structure by reducing the entropy because its pyrrolidine ring adopts fewer conformations than the corresponding Gln-62 residue in SVCP, as discussed for many other proteins previously (Matthews et al. 1987; Sriprapundh et al. 2000; Goihberg et al. 2007). In addition, the SBCP Lys-87 residue formed a salt bridge with Asp-91 on the

molecular surface, whereas the corresponding hydrophobic Val-87 residue in SVCP showed no interaction. Salt bridge formation on the molecular surface is reported to result in enhanced thermal stability of the proteins (Perl et al. 2000; Kuribayashi et al. 2017), whereas the hydrophobic residue on the molecular surface is reported to result in decreased thermal stability of the protein (Lee et al. 2005). Some of these specific structural differences may contribute to the higher thermal stability of SBCP than that of SVCP.

Thermal stability analysis of the SBCP variants

To verify the structural insights described above, thermal denaturation experiments were carried out for the SBCP variants, which had been mutated so as to have the corresponding SVCP residues, by means of CD spectral measurement. The normalized data for CD spectral changes at 222 nm during thermal denaturation were plotted as a function of temperature (Fig. 6). The T_m values during thermal denaturation of the SBCP Ala-43 to Thr (A43T), Pro-62 to Gln (P62Q), and Lys-87 to Val (K87V) variants were 55.6 ± 0.2 , 53.4 ± 0.2 , and 51.9 ± 0.4 °C, respectively, the mean and standard deviation values being obtained for three independent measurements.

Fig. 5 Structure comparison between SBCP (green) and SVCP (violet). The relevant amino acid residues are indicated



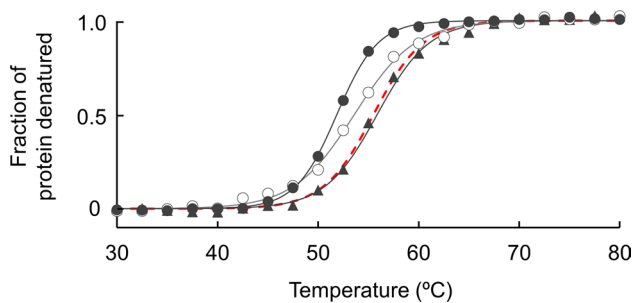


Fig. 6 Thermal stability profiles of the SBCP variants. The fractions of representative raw data are plotted at a temperature interval of 2.5 °C for the A43T (closed triangles), P62Q (open circles), and K87V (closed circles) variants. The fitting curves are also shown, and red dashed line is the fitting curve of thermal denaturation for the SBCP wild-type protein, which has been already shown in Fig. 4a in this paper

Among these variants, the T_m value of the A43T variant was essentially the same as that of the wild-type, and those of P62Q and K87V variants significantly decreased as compared with that of the wild-type. These results indicated that the molecular interior Ala-43 did not contribute to the SBCP stability as compared with SVCP, but the molecular surface Pro-62 and Lys-87 residues were responsible for the higher stability of SBCP, consistent with the structural prediction above.

Plausibly, the thermal stability difference between SBCP and SVCP can be related to the growth pressure of their source bacteria, psychrophilic *S. benthica* and *S. violacea*, growing optimally at 50 and 30 MPa, respectively. It could be possible that SBCP was more stable than SVCP because *S. benthica* is more piezophilic than *S. violacea*. However, there is presently no clear explanation about the relationship between the protein thermal stability and piezophilicity of source organism, presumably representing complex multiple adaptation to low temperature and high hydrostatic pressure. More information, together with those from other proteins (Hamajima et al. 2016, Fujii et al. 2018), should be collected for a better explanation of this relationship.

Conclusion

This study was aimed at further elucidation of the stability regulation in cytochromes *c'* previously observed in thermophilic and mesophilic ones, extending to psychrophilic ones using *Shewanella* cytochromes *c'*. As expected, together with the previous findings (Fujii et al. 2017), the stability of cytochromes *c'* from the psychrophile, mesophile, and thermophile is systematically regulated in molecular interior regions. An unanticipated observation in the present study was the stability difference between the SBCP and SVCP

proteins, which was attributed to the differences in the amino acid residues located on the molecular surface. As the psychrophilic sources of SBCP and SVCP are also piezophilic, the adaptation of these proteins to multiple extreme environments of low temperature and high hydrostatic pressure appears to be complex, which may be required for proper protein function in the source organisms.

Acknowledgements We would like to thank Daisuke Yamane-Koshizawa for his technical support and the discussion.

Funding This work was supported by Grants-in-Aid for Scientific Research from the Ministry of Education, Culture, Sports, Science and Technology of Japan (nos. 26240045 and 16K07692 to Y.S.), a Grant from the Japan Society for the Promotion of Science (no. 25–1446 to S.F.), a Grant-in-Aid for Young Human Resource Support from the Ministry of Education, Culture, Sports, Science and Technology in Japan (no. 1617PD0536 to S.F.), and a Grant-in-Aid for Fundamental Research from the Graduate School of Biosphere Science, Hiroshima University to S. F. L.L. is very grateful to the Indonesia Endowment Fund for Education, Ministry of Finance, Republic of Indonesia for the scholarship.

References

- Adams PD, Afonine PV, Bunkóczi G, Chen VB, Davis IW, Echols N, Headd JJ, Hung L, Kapral GJ, Grosse-Kunstleve RW, McCoy AJ, Moriarty NM, Oeffner R, Read RJ, Richardson DC, Richardson JS, Terwilliger TC, Zward PH (2010) PHENIX: a comprehensive Python-based system for macromolecular structure solution. *Acta Crystallogr Sect D Biol Crystallogr* 66:213–221
- Akanuma S, Nakajima Y, Yokobori S, Kimura M, Nemoto N, Mase T, Miyazono K, Tanokura M, Yamagishi A (2013) Experimental evidence for the thermophilicity of ancestral life. *Proc Natl Acad Sci USA* 110:11067–11072
- Ambler RP, Kamen MD, Bartsch RG, Meyer TE (1991) Amino acid sequences of *Euglena viridis* ferredoxin and cytochromes *c*. *Biochem J* 276:47–52
- Biasini M, Bienert S, Waterhouse A, Arnold K, Studer G, Schmidt T, Kiefer F, Cassarino TG, Bertoni M, Bordoli L, Schwede T (2014) SWISS-MODEL: modeling protein tertiary and quaternary structure using evolutionary information. *Nucleic Acids Res* 42:W252–W258
- Chen VB, Arendall WB, Headd JJ, Keedy DA, Immormino RM, Kapral GJ, Murray LW, Richardson JS, Richardson DC (2010) MolProbity: all-atom structure validation for macromolecular crystallography. *Acta Crystallogr D Biol Crystallogr* 66:12–21
- Chou PY, Fasman GD (1978) Empirical predictions of protein conformation. *Annu Rev Biochem* 47:251–276
- Emsley P, Cowtan K (2004) Coot: model-building tools for molecular graphics. *Acta Crystallogr D Biol Crystallogr* 60:2126–2132
- Fujii S, Masanari M, Inoue H, Yamanaka M, Wakai S, Nishihara H, Sambongi Y (2013) High thermal stability and unique trimer formation of cytochrome *c'* from thermophilic *Hydrogenophilus thermoluteolus*. *Biosci Biotechnol Biochem* 77:1677–1681
- Fujii S, Oki H, Kawahara K, Yamane D, Yamanaka M, Maruno T, Kobayashi Y, Masanari M, Wakai S, Nishihara H, Ohkubo T, Sambongi Y (2017) Structural and functional insights into thermally stable cytochrome *c'* from a thermophile. *Protein Sci* 26:737–748
- Fujii S, Masanari-Fujii M, Kobayashi S, Kato C, Nishiyama M, Harada Y, Wakai S, Sambongi Y (2018) Commonly stabilized

- cytochromes *c* from deep-sea *Shewanella* and *Pseudomonas*. *Biosci Biotechnol Biochem* 82:792–799
- Goihberg E, Dym O, Tel-Or S, Levin I, Peretz M, Burstein Y (2007) A single proline substitution is critical for the thermostabilization of *Clostridium beijerinckii* alcohol dehydrogenase. *Proteins* 66:196–204
- Goto E, Kodama T, Minoda Y (1977) Isolation and culture conditions of thermophilic hydrogen bacteria. *Agric Biol Chem* 41:685–690
- Gromiha MM, Oobatake M, Sarai A (1999) Important amino acid properties for enhanced thermostability from mesophilic to thermophilic proteins. *Biophys Chem* 82:51–67
- Hamajima Y, Nagae T, Watanabe N, Ohmae E, Kato-Yamada Y, Kato C (2016) Pressure adaptation of 3-isopropylmalate dehydrogenase from an extremely piezophilic bacterium is attributed to a single amino acid substitution. *Extremophiles* 20:177–186
- Holm HW, Vennes JW (1970) Occurrence of purple sulfur bacteria in a sewage treatment lagoon. *Appl Microbiol* 19:988–996
- Inoue H, Wakai S, Nishihara H, Sambongi Y (2011) Heterologous synthesis of cytochrome *c'* by *Escherichia coli* is not dependent on the System I cytochrome *c* biogenesis machinery. *FEBS J* 278:2341–2348
- Kato C, Sato T, Horikoshi K (1995) Isolation and properties of barophilic and barotolerant bacteria from deep-sea mud samples barotolerant bacteria from deep-sea mud samples. *Biodivers Conserv* 4:1–9
- Kato Y, Fujii S, Kuribayashi T, Masanari M, Sambongi Y (2015) Thermal stability of cytochrome *c'* from mesophilic *Shewanella amazonensis*. *Biosci Biotechnol Biochem* 79:1125–1129
- Kulakova L, Galkin A, Kurihara T, Yoshimura T, Esaki N (1999) Cold-active serine alkaline protease from the psychrotrophic bacterium *Shewanella* strain Ac10: gene cloning and enzyme purification and characterization. *Appl Environ Microbiol* 65:611–617
- Kuribayashi T, Fujii S, Masanari M, Yamanaka M, Wakai S, Sambongi Y (2017) Difference in NaCl tolerance of membrane-bound 5'-nucleotidases purified from deep-sea and brackish water *Shewanella* species. *Extremophiles* 21:357–368
- Lauro FM, Chastain RA, Ferreira S, Johnson J, Yayanos AA, Bartlett DH (2013) Draft genome sequence of the deep-sea bacterium *Shewanella benthica* strain KT99. *Genome Announc* 1:e00210–e00213
- Lee CF, Makhatadze GI, Wong KB (2005) Effects of charge-to-alanine substitutions on the stability of ribosomal protein L30e from *Thermococcus celer*. *Biochemistry* 44:16817–16825
- Manole A, Kekilli D, Svistunenko DA, Wilson MT, Dobbin PS, Hough MA (2015) Conformational control of the binding of diatomic gases to cytochrome *c'*. *J Biol Inorg Chem* 20:675–686
- Masanari M, Wakai S, Ishida M, Kato C, Sambongi Y (2014) Correlation between the optimal growth pressures of four *Shewanella* species and the stabilities of their cytochromes *c*₅. *Extremophiles* 18:617–627
- Matthews BM (1968) Solvent content of protein crystals. *J Mol Biol* 33:491–497
- Matthews BW, Nicholson H, Becktel WJ (1987) Enhanced protein thermostability from site-directed mutations that decrease the entropy of unfolding. *Proc Natl Acad Sci USA* 84:6663–6667
- McCoy AJ, Grosse-Kunstleve RW, Adams PD, WinnMD Storoni LC, Read RJ (2007) Phaser crystallographic software. *J Appl Crystallogr* 40:658–674
- Moore GR (1991) Bacterial 4- α -helical bundle cytochromes. *Biochim Biophys Acta* 1058:38–41
- Perl D, Mueller U, Heinemann U, Schmid FX (2000) Two exposed amino acid residues confer thermostability on a cold shock protein. *Nat Struct Biol* 7:380–383
- Sambongi Y, Ferguson SJ (1994) Synthesis of holo *Paracoccus denitrificans* cytochrome *c*₅₅₀ requires targeting to the periplasm whereas that of holo *Hydrogenobacter thermophilus* cytochrome *c*₅₅₂ does not. Implications for *c*-type cytochrome biogenesis. *FEBS Lett* 340:65–70
- Sambongi Y, Stoll R, Ferguson SJ (1996) Alteration of haem-attachment and signal-cleavage sites for *Paracoccus denitrificans* cytochrome *c*₅₅₀ probes pathway of *c*-type cytochrome biogenesis in *Escherichia coli*. *Mol Microbiol* 19:1193–1204
- Sambongi Y, Uchiyama S, Kobayashi Y, Igarashi Y, Hasegawa J (2002) Cytochrome *c* from a thermophilic bacterium has provided insights into the mechanisms of protein maturation, folding, and stability. *Eur J Biochem* 269:3355–3361
- Schuck P (2000) Size-distribution analysis of macromolecules by sedimentation velocity ultracentrifugation and Lamm equation modeling. *Biophys J* 78:1606–1619
- Scopes RK (1974) Measurement of protein by spectrophotometry at 205 nm. *Anal Biochem* 59:277–282
- Sriprapundh D, Vieille C, Zeikus JG (2000) Molecular determinants of xylose isomerase thermal stability and activity: analysis of thermozymes by site-directed mutagenesis. *Protein Eng* 13:259–265
- Takenaka S, Wakai S, Tamegai H, Uchiyama S, Sambongi Y (2010) Comparative analysis of highly homologous *Shewanella* cytochromes *c*₅ for stability and function. *Biosci Biotechnol Biochem* 74:1079–1083
- Uchiyama S, Ohshima A, Nakamura S, Hasegawa J, Terui N, Takayama SJ, Yamamoto Y, Sambongi Y, Kobayashi Y (2004) Complete thermal-unfolding profiles of oxidized and reduced cytochromes *c*. *J Am Chem Soc* 126:14684–14685
- Venkateswaran K, Dollhopf ME, Aller R, Stackebrandt E, Nealson KH (1998) *Shewanella amazonensis* sp. nov., a novel metal-reducing facultative anaerobe from Amazonian shelf muds. *Int J Syst Bacteriol* 48:965–972
- Yamane-Koshizawa D, Fujii S, Maruno T, Kobayashi Y, Yamanaka M, Wakai S, Sambongi Y (2018) Stabilization of mesophilic *Allochromatium vinosum* cytochrome *c'* through specific mutations modeled by a thermophilic homologue. *Biosci Biotechnol Biochem* 82:304–311